THE TGFβ PATHWAY STIMULATES OVARIAN CANCER CELL PROLIFERATION BY INCREASING IGF1R LEVELS

Elisenda Alsina-Sanchís[1,6], Agnès Figueras[1,6], Álvaro Lahiguera[1,6], August Vidal[2,3,6], Oriol Casanovas[1,6], Mariona Graupera[4], Alberto Villanueva[1,3,6], Francesc Viñals[1,5,6]

1 Program Against Cancer Therapeutic Resistance (ProCURE), Institut Català d'Oncologia (ICO), Hospital Duran i Reynals, 08908 L'Hospitalet de Llobregat (Barcelona), Spain; 2 Servei d'Anatomia Patològica, Hospital Universitari de Bellvitge, 08908 L'Hospitalet de Llobregat; 3 Xenopat S.L., Business Bioincubator, Bellvitge Health Science Campus, 08907 L'Hospitalet de Llobregat; 4 Laboratori d'Oncologia Molecular, Institut d'Investigació Biomèdica de Bellvitge (IDIBELL), 08908 L'Hospitalet de Llobregat; 5 Departament de Ciències Fisiològiques II, Universitat de Barcelona, Avda Feixa Llarga s/n 08907 L'Hospitalet de Llobregat and 6 Institut d'Investigació Biomèdica de Bellvitge (IDIBELL)

* To whom correspondence should be addressed.

Mailing address: Dr. Francesc Viñals - Program Against Cancer Therapeutic Resistance (ProCURE), Translational Research Laboratory, Institut Català d'Oncologia – IDIBELL, Hospital Duran i Reynals, Gran Via 199-203, 08908 L'Hospitalet de Llobregat, Barcelona, Spain. E-mail: fvinyals@iconcologia.net

Novelty and impact

In this work we describe, for first time, that high activation levels of the TGFβ pathway in epithelial ovarian cancers contributes to tumor ovarian cell proliferation by stimulating IGF1R expression. Our results have been obtained using orthotopic models of these tumors, human patient samples and ovarian tumoral cells, and lead us to propose the use of TGFβ inhibitors as an alternative to the use of IGF1R inhibitors for the treatment of epithelial ovarian cancers.

The authors declare no conflicts of interest.

ABSTRACT

In a search for new therapeutic targets for treating epithelial ovarian cancer we analyzed the Transforming Growth Factor Beta (TGFβ) signaling pathway in these tumors. Using a TMA with patient samples we found high Smad2 phosphorylation in ovarian cancer tumoral cells, independently of tumor subtype (high-grade serous or endometrioid). To evaluate the impact of TGFβ receptor inhibition on tumoral growth, we used different models of human ovarian cancer orthotopically grown in nude mice (OVAs). Treatment with a TGFβRI&II dual inhibitor, LY2109761, caused a significant reduction in tumor size in all these models, affecting cell proliferation rate. We identified Insulin Growth Factor (IGF)1 receptor as the signal positively regulated by TGFβ implicated in ovarian tumor cell proliferation. Inhibition of IGF1R activity by treatment with a blocker antibody (IMC-A12) or with a tyrosine kinase inhibitor (linsitinib) inhibited ovarian tumoral growth *in vivo*. When IGF1R levels were decreased by shRNA treatment, LY2109761 lost its capacity to block tumoral ovarian cell proliferation. At the molecular level TGFβ induced mRNA IGF1R levels. Overall, our results suggest an important role for the TGFβ signaling pathway in ovarian tumor cell growth through the control of IGF1R signaling pathway. Moreover, it identifies anti-TGFβ inhibitors as being of potential use in new therapies for ovarian cancer patients as an alternative to IGF1R inhibition.

3

INTRODUCTION

Ovarian cancer is the second most common gynecological cancer by incidence (≈6 per 100,000 individuals) and the fifth most common cause of cancer death in women in western countries [1]. More than 90% of ovarian tumors have an epithelial origin and can be classified into four main histological types: high-grade serous (70% of cases; the more aggressive type), endometrioid, mucinous and clear cell tumors [2]. Although progress has been made in the treatment of this cancer by improved surgical debulking and the introduction of platinum-taxane regimens of chemotherapy, the overall 5-year survival rate is only 29% in advanced-stage disease (80% of cases). This low survival rate is mainly because of intrinsic and acquired resistance to platinum-based chemotherapy [1,3]. Together, these observations highlight the importance of having a more detailed understanding of potential new targets.

A good candidate is the Transforming Growth Factor Beta (TGFβ) signaling pathway. TGFβs members (formed by TGFβ1, 2 and 3) signal through binding to their membrane serine/threonine kinase receptors TGFβRII and I, phosphorylation of intracellular effectors Smad2 and Smad3, formation of heterodimers phosphoSmad2/3 with Smad4, translocation to the nucleus and regulation of gene transcription [4, 5]. TGFβ members play a role as inhibitors of normal epithelial and endothelial cell proliferation, but they contribute to cancer progression in later stages. This dual role is caused by mutations that abrogate the normal cell cycle arrest caused by TGFβ members, but that maintain TGFβ–stimulation of the

4

processes involved in cancer progression and dissemination, such as EMT transition, angiogenesis, extracellular matrix remodeling, migration and invasion [6-8]. TGFβ plays a similar role in ovary. Thus, while TGFβ blocks cell growth in normal ovarian epithelial cells, in 40% of ovarian carcinomas TGFβ loses its cytostatic effect but maintains EMT induction and production of extracellular matrix [9]. Considering these data from ovarian cancer cells and that treatments against TGFβ are now under clinical development [10-12], we decided in this work to study the contribution of TGFβ to ovarian cancer progression using orthotopic models of ovarian cancer.

MATERIALS AND METHODS

Chemical compounds

LY2109761 was kindly provided by Lilly and Co. It was dissolved in 1% carboxymethylcellulose-0.5% sodium lauryl sulfate (Sigma)-0.085% Polyvinylpyrrolidone (Sigma)-0.05% antifoam (Sigma) solution. Drug aliquots were prepared every two weeks and kept in the dark at 4°C. IMC-A12 (Cixutumumab) was obtained from ImClone (NJ, USA). Linsitinib was obtained from LC Laboratories (MA, USA) and was dissolved in 25 mM tartaric acid (Sigma) solution. TGFβ was provided by R&D. Other reagents were purchased from Sigma or Roche.

5

Orthotopic implantation of ovarian tumors

Female NMRI-nu immunodeficient mice (strain NMRI-*Foxn1^{nu}/Foxn1^{nu}*) were purchased from Janvier (France). Mice were housed and maintained in laminar flow cabinets under specific pathogen-free conditions. All the animal studies were approved by the local committee for animal care (DAAM 5766).

The ovarian tumors used were perpetuated in nude mice by consecutive passages. We used three orthotopic ovarian patient-derived xenograft (PDX, also called Orthoxenografts) models. They were generated in our group by implantation into nude mice of tumor samples obtained from untreated patients after surgery. The study protocol was cleared by Ethics Committee of Bellvitge Hospital and a signed informed consent was obtained from each patient. PDX were one endometrioid tumor model (OVA15, from a 72 years old patient, FIGO stage I) and two high-grade serous ovarian tumor models, OVA8 (from a 47 years old patient, FIGO stage III) and OVA17 (from a 77 years old patient, FIGO stage III). At the histological level all three patient tumors were grade 3, but clinically (FIGO classification) OVA 15 was classified as Stage I while OVA 8 and OVA17 were classified as Stage III. At the mutational level, all three tumors present mutations in *TP53*. Moreover, OVA15 presents a mutation in *ARID1A*, while OVA8 presents a heterozygous STOP codon in *BRCA2* gene.

Patient that originated OVA17 already presented a big dissemination node (> 8 cm) and 15 para-aortic nodes. When implanted in mice this tumor generates macroscopic tumoral nodes in the peritoneal zone and liver metastasis. All the

OVA17 implanted in mice developed peritoneal dissemination after two months from implantation.

For surgical implantation mice were anesthetized by isoflurane inhalation. A small incision was made and the ovaries were exteriorized. A 6-mm^3 piece tumor was implanted in each ovary using Prolene 7.0 surgical sutures. The ovaries were returned to the abdominal cavity and the incision was closed with wound clips. Buprex was administered i.p. to the mice (200 μl) the day of the surgical intervention and for two days after the implantation.

Treatment schedule

As the tumors had different growth behaviors the treatment schedules were different. Treatments started when a palpable intra-abdominal mass was detected; studies were terminated when tumors in vehicle-treated animals were judged to be adversely affecting their wellbeing.

Treatment of the high-grade serous tumor models OVA8 and OVA17 started 5 weeks after implantation and continued for one further month. Treatment of the OVA15 endometrial model started six weeks after tumor implantation and continued for another month more. Mice were treated with LY2109761, administered twice daily with gavage as an oral dose of 100 mg/kg [13]. Control mice were treated with the vehicle oral solution as the treated groups.

These treatments had no significant effect on mouse body weight and the animals appeared healthy and active throughout the study.

Linsitinib treatment of OVA8 started 4 weeks after implantation. Linsitinib was administered daily (5 days) with an oral dose of 40 mg/kg by gavage [14], 1 week without treatment followed by a new cycle of treatment for 5 days. Control mice were treated with the vehicle oral solution as the treated groups.

IMC-A12 (Cixutumumab) treatment of OVA17 started 5 weeks after implantation. The antibody was administered i.p. three times a week for 4 weeks at a dose of 12 mg/kg.

After sacrifize the effects of the different treatments on tumor response were evaluated by determining tumor weight and volume, where volume = (length)(width^2/2).

The rest of the methods are described in the Supplementary Materials and Methods.

RESULTS

To explore the importance of the TGFβ signaling pathway in ovarian cancer, we first performed immunohistochemical analysis for active Smad2 levels (phosphoSmad2 or pSmad2), instead of using total protein levels. We used a TMA

containing 32 high-grade serous and 34 endometrioid primary tumors obtained from patients affected by these ovarian cancers. As observed in Fig. 1A, the main part of the tumors were stained for pSmad2 at high levels, all of them presenting nuclear localization as expected for active pSmad2. No differences in pSmad2 were found when comparing high-grade serous with endometrioid tumors (Fig. 1B). We detected high activation levels of pSmad2 in the epithelium of normal human Fallopian tube compared with parenchymal cells (Fig. 1C). These epithelial cells are mainly the origin of epithelial high-grade serous tumoral ovarian cells [15, 16], indicating that these tumoral cells maintain a pathway that is already active in normal physiology.

The previous results prompted us to investigate the role of the TGFβ pathway for ovarian cancer progression in both tumors subtypes in greater depth. To this end we used orthotopic pre-clinical models generated after implantation in nude mice of tumors samples obtained from patients after surgery (PDX or orthoxenografts), two high-grade serous ovarian tumors (OVA8 and OVA17) and OVA15, an endometrioid ovarian tumor model. We confirmed the results of high pSmad2 levels in normal epithelial cells from human samples in those of normal mouse Fallopian tube (Fig. 1C). We also observed that the PDX orthotopic models presented a high degree of nuclear pSmad2 staining, very similar to the expression pattern found in primary tumors (Fig. 1C).

In order to block activation of the TGFβ pathway in these models we measured the effect of an inhibitor of TGFβRI and II kinase activity, LY2109761 [17]

9

that had previously showed inhibitory effects on ovarian cancer cells [18], on the growth of orthotopic ovarian tumors. After tumor implantation, mice bearing these tumors were randomized into two groups, and when a palpable intra-abdominal mass was detected, animals were treated with the vehicle or LY2109761 for 1 month. The treatments had no significant effect on mouse body weight and the animals appeared healthy and active throughout the study. LY2109761 treatment reduced tumor growth in all the tumor models tested (Fig. 2A): OVA17 (tumor volume: 1337 mm^3 in control versus 537 mm^3 in treated), OVA8 (control, 1088 mm^3 versus treated, 583 mm^3) and OVA15 (control, 2291 mm^3 versus treated, 991 mm^3). The effectiveness of the TGFβ inhibition was verified by western blot of tumor samples. A reduction in the levels of pSmad2 after LY2109761 treatment was observed in all the tumors treated (Fig. 2B). Surprisingly, the LY2109761 treatment only inhibited tumor growth; it had no effect on the capacity of the tumor to disseminate to other organs (Supplementary Fig. 1A).

The above results prompted us to determine how LY2109761 reduced tumor volume. We focused our study on OVA17 tumor samples as it was the one with the most statistically significant reduction in tumour volume. Our results showed that tumor size reduction was not due to an increase in apoptosis or necrosis (Supplementary Fig. 1B and C), ruling out the possibility of an effect of the treatment increasing cell death, or to changes in angiogenesis (Supplementary Fig. 1D). Subsequently, we examined whether cell proliferation became blocked by inhibition of the TGFβ pathway. With this objective, sections of control and treated tumor samples from OVA17 were stained with Ki67. LY2109761 treatment caused

10

a significant decrease in the proliferation rate (Fig. 2C). This effect on proliferation was also observed in the other tumoral models (OVA8 and OVA15, Fig. 2C). To confirm this effect we analyzed several proteins and signaling pathways involved in the control of cell proliferation. We did not detect any change in active or total AKT levels when comparing samples from control and LY2109761-treated OVA17 tumors (Fig. 2D and Supplementary Fig. 2A). In contrast, active ERK1/2 levels were decreased by 38% with LY2109761 treatment (Fig. 2D and Supplementary Fig. 2B). This effect was also observed in OVA8 treated tumors (Supplementary Fig. 2B). Next we checked proteins directly involved in cell cycle progression. We found no change in p21 or Cyclin A, although an increase in p16 (70%) and in E-Cadherin (350%) protein levels were noted (Fig. 2E and Supplementary Fig. 2C and 2D). In contrast, Cyclin D1 levels (measured by immunohistochemistry) were decreased by 60% in tumors treated with LY2109761 (Fig. 2F).

As the TGFβ signaling pathway by itself is not a classical stimulator of cell proliferation, we thought that this effect could be mediated by a different factor that is regulated by TGFβ. Equivalent mechanisms have already been described, for example in gliomas, in which inhibition of TGFβ reduced the size of tumors by affecting PDGF-B production and PDGFRβ-signaling pathways[19]. To establish whether this was also the case in ovarian tumors, we checked the expression of members of the PDGF family (PDGF-A, PDGF-B, PDGFRα and PDGFRβ) at the mRNA level, but found no difference between the groups (Supplementary Fig. 3A-D). Some other receptors from proliferation pathways like HER/ERBR family

11

compartments (Fig. 3C). We used our TMA containing samples from various patients affected by ovarian cancers to analyze IGF1R expression. As seen in Fig. 3D, and similarly to the pSmad2 staining, the main part of the tumors presented high levels of IGF1R. More strikingly, we found a significant correlation between the levels of pSmad2 and IGF1R in the same serous tumor (Fig. 3E). These results indicate that IGF1R expression is dependent on the activation of the TGFβ-Smad2 pathway.

Next, we decided to study the importance of IGF1R in our ovarian tumor cancer models. To this end, we treated OVA17 tumors with IMC-A12 (Cixutumumab), a monoclonal antibody against IGF1R that blocks the activity of this receptor. Treatment for 4 weeks with this antibody caused an 8% decrease in body weight of the animals. Given these side effects, antibody treatment caused a 42% decrease in tumor size (control tumors, 1225 mm^3 versus treated tumors, 713 mm^3) (Fig. 4A), indicating the great importance of this signaling pathway in this ovarian cancer model. We also tested linsitinib (OSI-906), a tyrosine kinase inhibitor specific for IGF1R and insulin receptor [14, 22] on OVA8 growth. In this case we also observed side effects on mice body growth (14% decrease after 1 week of treatment). For this reason, we administer linsitinib in an alternating regimen of two cycles of 5 days treatment followed by 7 days off. In all, animals were treated or not with linsitinib for 10 days. At the end of the treatment, treated animals presented a 14% decrease in body weight. Even considering these toxic effects, however, linsitinib caused a 60% decrease in tumor volume (controls, 1500 mm^3 versus treated, 600 mm^3; Fig. 4B).

13

The question arises as to how the TGFβ pathway affects IGF1R levels. To answer this first we measured IGF1R mRNA levels in the various treated and untreated orthotopic tumors. As observed in Fig. 5A, LY2109761 treatment caused a decrease in IGF1R mRNA levels in OVA8 and OVA15 tumors, while no effect was observed in OVA17, implying that several TGFβ-stimulated mechanisms control IGF1R levels. Next, we used cell culture ovarian tumoral models to analyze for IGF1R expression and TGFβ stimulation. Of the cell lines analyzed, the A2780 and OV90 ovarian serous cell types responded well to TGFβ stimulating Smad3 phosphorylation, effect that was inhibited by LY2109761 (Fig. 5B and Supplementary Fig. 4A). We evaluated in these cells the effect of LY2109761 inhibitor on cell viability. Addition of LY2109761 caused a dose-response inhibition in the number of viable cells (Fig. 5C and Supplementary Fig. 4B). We also incubated cells in the presence of IMC-A12 antibody. Results also indicated a reduction in cell viability caused by IMC-A12 incubation, similar results to the obtained in tumors. We measured IGF1Rβ protein levels in A2780 cells treated for 24 h with TGFβ or LY2109761. TGFβ caused a 100% increase in IGF1Rβ levels, while LY2109761 treatment caused a 23% decrease in this protein (Fig. 5D). Analysis of mRNA expression of members of the IGFs signaling pathway (e.g., IGF1, IGF1R and IGF1 binding proteins) revealed a TGFβ stimulation and LY2109761 inhibition of IGF1R mRNA levels in A2780 cells (Fig. 5E). Overall, these results suggest a transcriptional mechanism involved in controlling IGF1R levels, which is consistent with the results obtained from OVA8 and OVA15 orthotopic tumor models.

14

A further question arises as to how important IGF1R is in the observed LY2109761-effect. To address this issue, we inhibited IGF1R expression in A2780 and OV90 cells. By transducing lentiviral vectors expressing either IGF1R-shRNAs or a negative control using a non-silencing vector, A2780- or OV90-NS and A2780- or OV90-shIGF1R cells were generated. We used three independent shRNA vectors. Two of them (shV2-71 and shV2-72) reduced IGF1Rβ protein expression by 70-90% (Fig. 6A and Supplementary Fig. 4C), while the shV2-48 vector only reduced expression by 30%. This IGF1Rβ protein depletion caused a reduction in pERK1/2 levels (Fig. 6A and Supplementary Fig. 4C). As shown in Fig. 6B, the decrease of IGF1Rβ levels in A2780 cells reduced cell number in proportion to the IGF1Rβ levels still expressed: 70% inhibition in shV2-71 and shV2-72, but no reduction in shV2-48. In order to determine whether the LY2109761 effect was IGF1R-dependent, we added LY2109761 inhibitor to A2780-NS cells and to A2780-shIGF1R cells. Inhibition of IGF1Rβ expression caused a loss of LY2109761 sensitivity (Fig. 6C), indicating that IGF1R expression was critical for the LY2109761 effect. The same results were obtained in OV90 cells (Supplementary Fig. 4D).

15

DISCUSSION

Our results show that TGFβ plays an important role in proliferation of epithelial ovarian tumoral cells through the positive regulation of IGF1R protein levels. An active TGFβ signaling pathway is characteristic of later stages of tumoral proliferation, as in squamous cell carcinomas[23] or gliomas[19]. In these latter tumors, high pSmad2 is correlated with poor prognosis. For this reason, different targeted drugs have been developed against this pathway, some of which are currently in clinical trials [10-12]. It has recently been described that in advanced serous ovarian cancers pSmad2 staining is also correlated with poor patient outcome [24]. Our results confirmed the activation of the canonical TGFβ signaling pathway (high Smad2 phosphorylation) on ovarian carcinomas and with independence of their anatomical origin (high-grade serous or endometrioid). PSmad2 is present in tumoral cells, with only a few positive stromal cells. Our results also indicate that ovarian epithelial tumors maintain the activity of the TGFβ-Smad2/3 pathway, which is already active in normal Fallopian tube epithelium. In fact, this pathway also plays a positive role for granulosa cell proliferation during normal ovarian physiology [25, 26].

Our results suggest that IGF1R mediates the TGFβ effects on proliferation in ovarian cancer cells. IGF1R, a member of the insulin superfamily of growth promoting factors, has been implicated in the progression of many tumors controlling cell growth and proliferation [27, 28]. This TGFβ-IGF1R link is supported by the observed correlation between pSmad2 and total IGF1R levels in our orthotopic

16

models and in the TMA analyzed here. Control of IGF1R levels by TGFβ includes control of its mRNA levels probably through transcriptional mechanisms involving Smads, given that Smad binding sites are present in the conserved promoter region of the human IGF1R gene. Our results also identify that in OVA17 tumor IGF1R mRNA is not affected by TGFβ, implicating alternative post-translational mechanisms. However, the important point is that TGFβ always positively controls IGF1R levels in ovarian cancer cells. Positive effects of TGFβ on the IGF1R pathway have been described in osteosarcoma cells, where TGFβ increases IGFBP-3 protein, in turn boosting IGF1R signaling [29]. In normal prostate cells the IGF axis and TGFβ are both upregulated during normal prostate epithelial differentiation, and downregulated in local prostate cancer. After TGFβ treatment, the expression of the IGF axis was enhanced in prostate cells expressing TGFβ receptors [30]. But to our knowledge, this is one of the first times that TGFβ has been shown to directly control IGF1R protein levels in tumoral cells. However, similar indirect mechanisms of control of cell growth and proliferation by TGFβ through other growth factors have been described, for example, in glioma models, where TGFβ stimulates production of PDGF-B and activation of PDGFRβ [19].

As indicated, IGF1R plays a role in the progression of various cancers, including those of the ovary [27,28]. For this reason, several clinical trials are evaluating the effect of IGF1R inhibitors in different tumors, including ovarian cancers. Some clinical trials have given modest results and some of these inhibitors proved to be toxic. We obtained the same result in our mouse

17

experiments treating animals with inhibitors against IGF1R, the blocking antibody IMC-A12 (Cixutumumab) and linsitinib (OSI-906), an inhibitor of the tyrosine kinase of the insulin and IGF1 receptors. Both treatments decreased mouse weight by 8-14%. Taking these unwanted effects into account, our results indicate that TGFβ inhibitors could be considered to be a treatment that is less toxic while producing similar anti-tumoral effects, at least in ovarian carcinomas. Over all, our results indicate that inhibitors of the TGFβ pathway could be a therapeutic alternative for the treatment of ovarian tumors in which the IGF1R plays a key role.

ACKNOWLEDGEMENTS

BIBLIOGRAPHY

1. Bast RC, Jr., Hennessy B, Mills GB. The biology of ovarian cancer: new opportunities for translation. Nat Rev Cancer 2009;9:415-28.

2. Vaughan S, Coward JI, Bast RC, Jr., Berchuck A, Berek JS, Brenton JD, Coukos G, Crum CC, Drapkin R, Etemadmoghadam D, Friedlander M, Gabra H, et al. Rethinking ovarian cancer: recommendations for improving outcomes. Nat Rev Cancer 2011;11:719-25.

3. Bowtell DD. The genesis and evolution of high-grade serous ovarian cancer. Nat Rev Cancer 2010;10:803-8.

4. Massague J. TGF-beta signal transduction. Annu Rev Biochem 1998;67:753-91.

5. Shi Y, Massague J. Mechanisms of TGF-beta signaling from cell membrane to the nucleus. Cell 2003;113:685-700.

6. Massague J, Gomis RR. The logic of TGFbeta signaling. FEBS Lett 2006;580:2811-20.

7. Massague J. TGFbeta in Cancer. Cell 2008;134:215-30.

8. Ikushima H, Miyazono K. TGFbeta signalling: a complex web in cancer progression. Nat Rev Cancer 2010;10:415-24.

9. Helleman J, Jansen MP, Burger C, van der Burg ME, Berns EM. Integrated genomics of chemotherapy resistant ovarian cancer: a role for extracellular matrix, TGFbeta and regulating microRNAs. Int J Biochem Cell Biol 2010;42:25-30.

10. Seoane J. The TGFBeta pathway as a therapeutic target in cancer. Clin Transl Oncol 2008;10:14-9.

11. Akhurst RJ, Hata A. Targeting the TGFbeta signalling pathway in disease. Nat Rev Drug Discov 2012;11:790-811.

12. Neuzillet C, Tijeras-Raballand A, Cohen R, Cros J, Faivre S, Raymond E, de Gramont A. Targeting the TGFbeta pathway for cancer therapy. Pharmacol Ther 2015;147:22-31.

13. Anido J, Saez-Borderias A, Gonzalez-Junca A, Rodon L, Folch G, Carmona MA, Prieto-Sanchez RM, Barba I, Martinez-Saez E, Prudkin L, Cuartas I, Raventos C, et al. TGF-beta Receptor Inhibitors Target the CD44(high)/Id1(high) Glioma-Initiating Cell Population in Human Glioblastoma. Cancer Cell 2010;18:655-68.

14. Leiphrakpam PD, Agarwal E, Mathiesen M, Haferbier KL, Brattain MG, Chowdhury S. In vivo analysis of insulin-like growth factor type 1 receptor humanized monoclonal antibody MK-0646 and small molecule kinase inhibitor OSI-906 in colorectal cancer. Oncol Rep 2013;31:87-94.

15. Levanon K, Crum C, Drapkin R. New insights into the pathogenesis of serous ovarian cancer and its clinical impact. J Clin Oncol 2008;26:5284-93.

16. Kurman RJ, Shih Ie M. The origin and pathogenesis of epithelial ovarian cancer: a proposed unifying theory. Am J Surg Pathol 2010;34:433-43.

17. Melisi D, Ishiyama S, Sclabas GM, Fleming JB, Xia Q, Tortora G, Abbruzzese JL, Chiao PJ. LY2109761, a novel transforming growth factor beta receptor type I and type II dual inhibitor, as a therapeutic approach to suppressing pancreatic cancer metastasis. Mol Cancer Ther 2008;7:829-40.

18. Gao Y, Shan N, Zhao C, Wang Y, Xu F, Li J, Yu X, Gao L, Yi Z. LY2109761 enhances cisplatin antitumor activity in ovarian cancer cells. Int J Clin Exp Pathol 2015;8:4923-32.

19. Bruna A, Darken RS, Rojo F, Ocana A, Penuelas S, Arias A, Paris R, Tortosa A, Mora J, Baselga J, Seoane J. High TGFbeta-Smad activity confers poor prognosis in glioma patients and promotes cell proliferation depending on the methylation of the PDGF-B gene. Cancer Cell 2007;11:147-60.

20. Shao M, Hollar S, Chambliss D, Schmitt J, Emerson R, Chelladurai B, Perkins S, Ivan M, Matei D. Targeting the insulin growth factor and the vascular endothelial growth factor pathways in ovarian cancer. Mol Cancer Ther 2012;11:1576-86.

21. Banerjee S, Kaye SB. New strategies in the treatment of ovarian cancer: current clinical perspectives and future potential. Clin Cancer Res 2013;19:961-8.

22. Buck E, Gokhale PC, Koujak S, Brown E, Eyzaguirre A, Tao N, Rosenfeld-Franklin M, Lerner L, Chiu MI, Wild R, Epstein D, Pachter JA, et al. Compensatory insulin receptor (IR) activation on inhibition of insulin-like growth factor-1 receptor (IGF-1R): rationale for cotargeting IGF-1R and IR in cancer. Mol Cancer Ther 2010;9:2652-64.

23. Oshimori N, Oristian D, Fuchs E. TGF-beta promotes heterogeneity and drug resistance in squamous cell carcinoma. Cell 2015;160:963-76.

24. Parikh A, Lee C, Joseph P, Marchini S, Baccarini A, Kolev V, Romualdi C, Fruscio R, Shah H, Wang F, Mullokandov G, Fishman D, et al. microRNA-181a has a critical role in ovarian cancer progression through the regulation of the epithelial-mesenchymal transition. Nat Commun 2014;5:2977.

25. Li Q, Pangas SA, Jorgez CJ, Graff JM, Weinstein M, Matzuk MM. Redundant roles of SMAD2 and SMAD3 in ovarian granulosa cells in vivo. Mol Cell Biol 2008;28:7001-11.

26. Richards JS, Pangas SA. The ovary: basic biology and clinical implications. J Clin Invest 2010;120:963-72.

27. Pollak M. The insulin and insulin-like growth factor receptor family in neoplasia: an update. Nat Rev Cancer 2012;12:159-69.

28. Bruchim I, Werner H. Targeting IGF-1 signaling pathways in gynecologic malignancies. Expert Opin Ther Targets 2013;17:307-20.

29. Schedlich LJ, Yenson VM, Baxter RC. TGF-beta-induced expression of IGFBP-3 regulates IGF1R signaling in human osteosarcoma cells. Mol Cell Endocrinol 2013;377:56-64.

30. Massoner P, Ladurner Rennau M, Heidegger I, Kloss-Brandstatter A, Summerer M, Reichhart E, Schafer G, Klocker H. Expression of the IGF axis is decreased in local prostate cancer but enhanced after benign prostate epithelial differentiation and TGF-beta treatment. Am J Pathol 2011;179:2905-19.

FIGURE LEGENDS

Figure 1. Epithelial ovarian tumors present high levels of pSmad2.

A) Examples representative of low (a), moderate (b) and high (c) levels of positive pSmad2 immunostaining in ovarian cancer patient samples.

B) Quantification of pSmad2 levels (using the multiplicative index of the stain intensity and the labeling frequency) in tumor tissue sections from high-grade serous or endometrioid tumor patients. Data analyzed from 66 tumor patients.

C) Hematoxylin-eosin (c, d, g and h), pSmad2 (a, b, e, f, i and j) staining of normal Fallopian tube epithelium (human, a or mouse, b), the original human tumor biopsy (c, e, g and i), OVA17 (d and f) and OVA15 (h and j) orthotopic tumors. a-j 400x, bar 100 µm. K and L amplifications at 630x of f and j, bar 20 µm.

Figure 2. Blocking of TGFβR activity inhibits tumor growth in three xenograft orthotopic models of epithelial ovarian tumors

A) Mice with orthotopically implanted OVA15, OVA8 or OVA17 ovarian tumors were treated with vehicle (5, 6 and 9 mice, respectively) or twice daily with 100 mg/kg LY2109761 (4, 6 and 9 mice, respectively) for four weeks. Mice were sacrificed when control mouse tumors affected the wellbeing of the animals. Final volumes are illustrated by a boxplot. *, $p < 0.05$; **, $p < 0.01$ (two-tailed Mann-Whitney U test).

22

B) Expression of pSmad2 and tubulin were analyzed by western blot in LY2109761-treated and control tumors. A representative blot showing results obtained for 3 independent OVA15 control tumors and 3 independent OVA15 LY2109761-treated tumors is shown. Densitometric quantifications of phosphoSmad2 relative to tubulin are shown. Results are the mean ± SEM of 5 controls and 6 LY-treated tumors in OVA15, 4 controls and 6 treated for OVA8 and 4 control tumors and 3 LY2109761-treated tumors in OVA17. Results are presented in arbitrary units relative to the control group. *, p < 0.05 (Mann-Whitney U test).

C) Sections from control and treated OVA15, OVA 8 and OVA17 tumors were stained for the proliferation marker Ki67. Quantification of the percentage of tumor Ki67-positive cells is shown. Results are the mean ± SEM of 4 controls and 3 LY-treated tumors in OVA15, 6 controls and 6 treated for OVA8 and 4 control tumors and 8 LY2109761-treated tumors in OVA17. **, p < 0.01 (two-tailed Mann-Whitney U test).

D) Expression of phosphorylated AKT (p-AKT), total AKT, phosphorylated ERK1/2 (p-ERK1/2), total ERK1/2 and tubulin was analyzed by western blot in OVA17 LY2109761-treated and control tumors. A representative blot showing results from two independent control tumors and four independent LY2109761-treated tumors.

E) Expression of E-cadherin, Cyclin A, p21, p16 and tubulin was analyzed by western blot in OVA17 LY2109761-treated and control tumors. A representative

23

blot showing results from 2 independent control tumors and 2 independent LY2109761-treated tumors is shown.

F) Sections from OVA17 control and treated tumors were stained for cyclin D1. Quantification of tumor cyclin D1-positive cells is expressed relative to the control group. Results are the mean ± SEM of 3 controls and 5 LY2109761-treated tumors. *, $p < 0.05$ (two-tailed Mann-Whitney U test).

Figure 3. IGF1R protein levels decrease after LY2109761 treatment

A) Phosphorylation levels of various RTKs were analyzed using a human phospho-RTK array kit in LY2109761-treated and control OVA17 tumors. Results are the mean of 2 control tumors and 2 LY2109761-treated tumors, and are represented in arbitrary units (after densitometric quantification) relative to the control group.

B) Total IGF1Rβ and vinculin expression was analyzed by western blotting in independent OVA17, OVA8 and OVA15 tumors from the treatments with vehicle or LY2109761. Representative blots show the results obtained. Densitometric quantifications of IGF1Rβ relative to vinculin are shown. Results are the mean ± SEM of 4 control tumors and 4 LY2109761-treated tumors in OVA17 (∗, $p < 0.05$, two-tailed Mann-Whitney U test), 3 controls and 3 treated for OVA8 (∗, $p < 0.05$, T-test) and 4 controls and 3 LY-treated tumors in OVA15. Results are presented in arbitrary units relative to the control group.

24

C) Histological IGF1R staining of OVA17 orthotopic tumors. Total (top) or membrane localized (down, indicated with arrows) 400x, bar 100 µm. Quantification of IGF1R total levels (top) or present in membrane (bottom) in tumor tissue sections from OVA17 control or LY2109761-treated samples. Results are the mean ± SEM of from 6 controls and 7 treated samples. ∗, p < 0.05, two-tailed Mann-Whitney U test.

D) Quantification of IGF1R levels (using the multiplicative index of the intensity of the stain and the labeling frequency) in tumor tissue sections from high-grade serous or endometrioid tumor patients. Data are from 65 tumor patients.

E) Correlation between pSmad2 and total IGF1R levels in tissue microarray from high-grade serous ovarian patients analyzed in Fig. 1B and Fig. 4D. The Spearman correlation coefficient is shown.

Figure 4. Blocking IGF1R activity inhibits tumor growth

A) Mice with an orthotopically implanted OVA17 tumor were treated with vehicle (6 mice) or the antibody IMC-A12 i.p. three times a week for 4 weeks at a dose of 12 mg/kg (4 mice). Mice were sacrificed when control mouse tumors affected the wellbeing of the animals. Final volumes are illustrated by a boxplot.

B) Mice with an orthotopically implanted OVA8 tumor were treated with linsitinib with an oral dose of 40 mg/kg by gavage (as indicated in results) to six mice. Eight mice were treated with the vehicle orally. Mice were sacrificed when control mouse

tumors affected the wellbeing of the animals. Final volumes are illustrated by a boxplot. *, $p < 0.05$ (Mann-Whitney U test).

Figure 5. TGFβ stimulates IGF1R mRNA and protein

A) mRNA levels of human IGF1R analyzed by quantitative real-time PCR in OVA17 (4 control tumors and 5 LY2109761-treated tumors), OVA8 (4 control and 3 LY-treated tumors samples) and OVA15 (5 control tumors and 3 LY2109761-treated tumors) orthotopic ovarian tumors. Results are expressed as the mean and SEM of mRNA expression relative to the control group. *, $p < 0.05$ (Mann-Whitney U test).

B) Exponential A2780 cells were incubated for 30 min in the absence (DMSO) or presence of TGFβ or TGFβ and 2 μM LY2109761. Cells were lysed and phosphoSmad3, total Smad2/3 and β-Actin expression was analyzed by western blot. A blot representative of three independent experiments is shown.

C) A2780 cells incubated for 5 days in the presence of the indicated concentrations of LY2109761, 50 μg/ml IMC-A12 or in the absence (DMSO). Cell viability was measured by MTT assay. Results are expressed relative to the control condition. Each data point represents the mean and SEM of five independent determinations. Differences between control and treated cases were considered statistically significant when $p < 0.05$ (*) or $p < 0.01$ (**) (two-tailed Mann-Whitney U test).

D) Expression of IGF1Rβ and β-Actin, as a loading control, were analyzed by western blot of A2780 cells lysates. Cells were incubated for 24 h with DMSO, TGFβ1 (10 ng/ml) or LY2109761 (2 µM). A representative blot of the results is shown.

E) mRNA levels of human IGF1R, IGF2R, IGF1 and IGF2 were analyzed by quantitative real-time PCR in A2780 (4 samples) cells incubated for 8 or 24 h with DMSO, TGFβ1 (10 ng/ml) or LY2109761 (2 µM). Results are expressed as the mean and SEM of mRNA expression relative to control condition. *, p < 0.05 (two-tailed Mann-Whitney U test).

Figure 6. IGF1R mediates LY2109761 effect.

A) IGF1Rβ, phosphorylated ERK1/2 (pERK1/2), total ERK1/2 and tubulin protein levels were analyzed by western blot in A2780-sh-NS, A2780-sh71, A2780-sh72 or A2780-sh48 cell lysates. A blot representative of three independent experiments is shown.

B) 5000 A2780-sh-NS, A2780-sh71, A2780-sh72 or A2780-sh48 cells were incubated for 3 days in normal medium, trypsinized and the number of cells was counted. Each data point represents the mean and SEM of 3 independent determinations. p < 0.05 (*) (T-test).

C) A2780-sh-NS, A2780-sh71, A2780-sh72 or A2780-sh48 cells were incubated for 5 days in the presence of the indicated concentrations of LY2109761 or in the

27

absence (DMSO). Cell viability was measured by MTT assay. Results are expressed as percentage relative to the control condition. Each data point represents the mean and SEM of three independent determinations. *, $p < 0.05$ (Mann-Whitney U test).
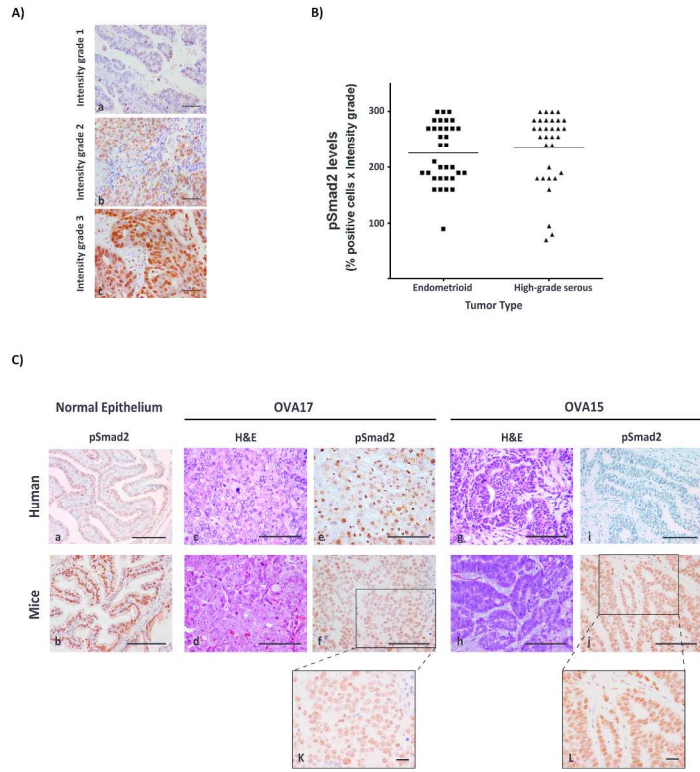
28

Figure 1

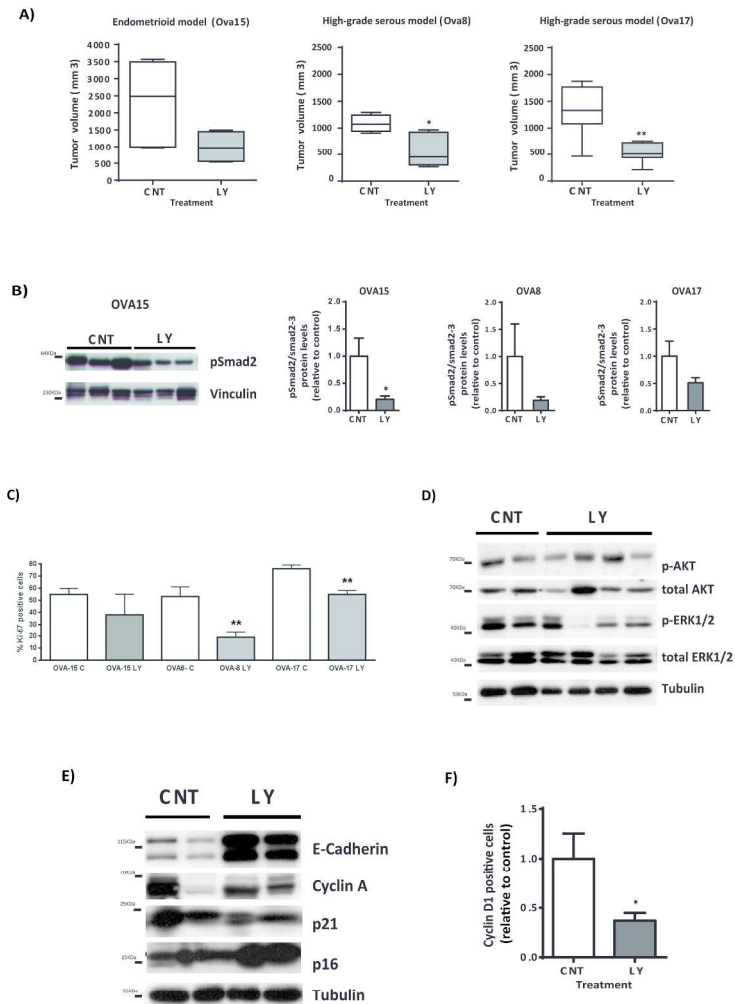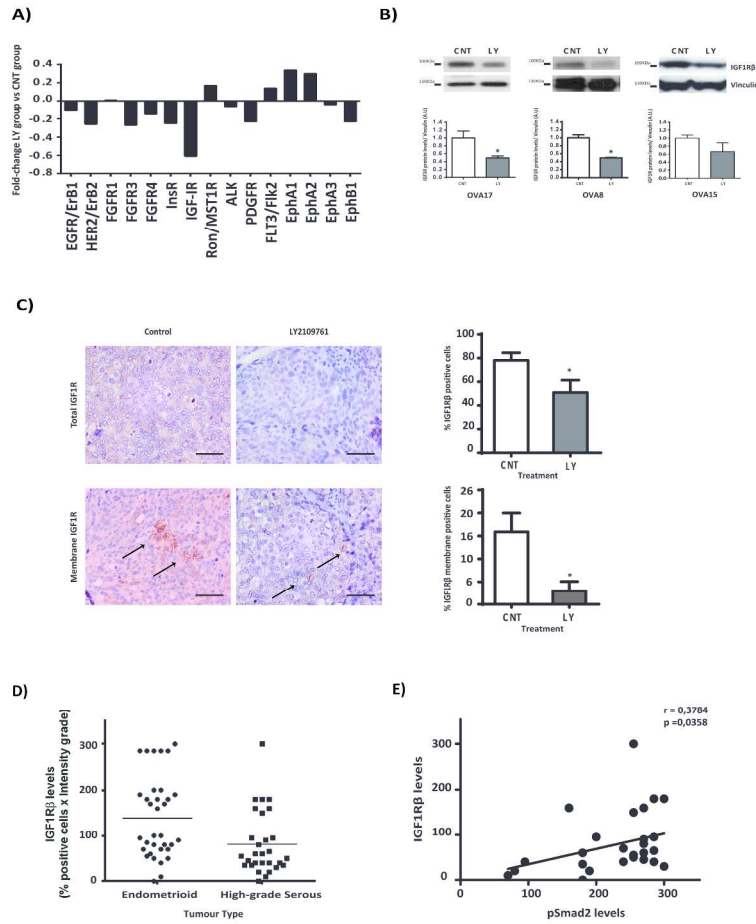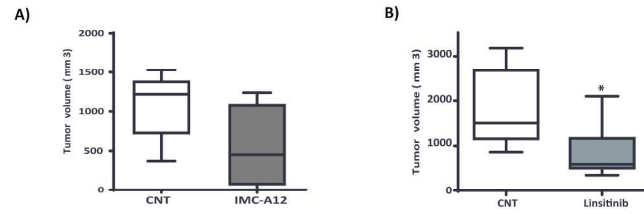

Figure 1
210x297mm (300 x 300 DPI)

Figure 2

Figure 2
210x297mm (300 x 300 DPI)

Figure 3

Figure 3
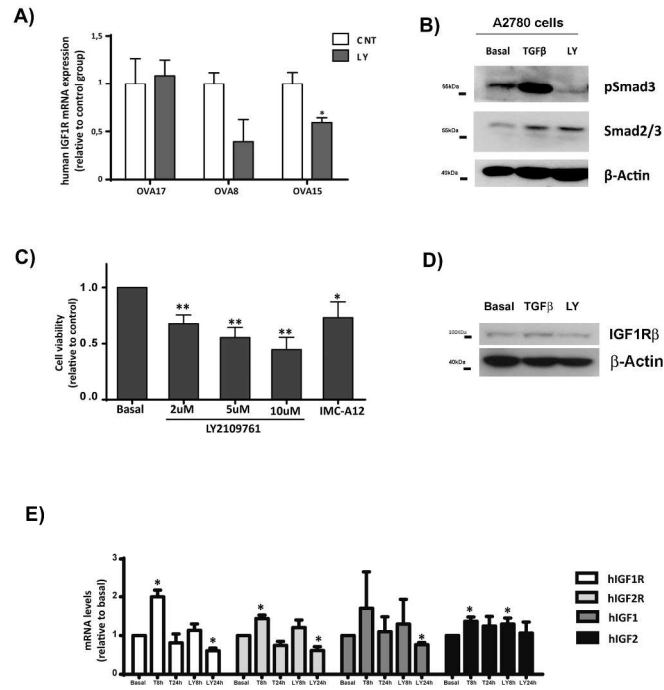210x297mm (300 x 300 DPI)

Figure 4

Figure 4
210x297mm (300 x 300 DPI)

Figure 5

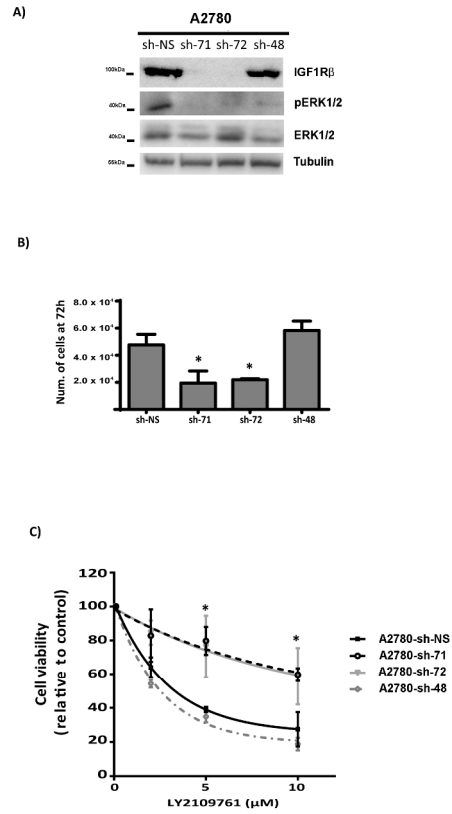
Figure 5
209x297mm (300 x 300 DPI)

Figure 6

A)

B)

C)

Figure 6
209x297mm (300 x 300 DPI)